ELSEVIER

Correlation between PAMPA permeability and cellular activities of hepatitis C virus protease inhibitors

*Cheng Li, Latha Nair, Tongtong Liu, Fangbiao Li, John Pichardo, Sony Agrawal, Robert Chase, Xiao Tong, Annette S. Uss, Stephane Bogen, F. George Njoroge, Richard A. Morrison, K.-C. Cheng** *

Schering-Plough Research Institute, K-15-2-2700, 2015 Galloping Hill Road, Kenilworth, NJ 07033, USA

ARTICLE INFO

ABSTRACT

Parallel artificial membrane permeability assay (PAMPA) and Caco-2 cells have been frequently used for the evaluation of in vitro permeability of new chemical entities. In this study we evaluated the correlation between permeability, assessed by both methods, and the cellular potency of 34 novel hepatitis C virus (HCV) protease inhibitors. Two types of assays were used to determine the potency of HCV protease inhibitors: a cell-free assay that evaluates the intrinsic affinity (K_i) between the protease and the inhibitor and a cell-based replicon assay that determines the inhibitors' IC_{90}. When the K_i/IC_{90} ratios were compared with the PAMPA permeability and the Caco-2 permeability by linear regression analysis, a reasonable correlation was found between the K_i/IC_{90} ratio and PAMPA permeability ($r^2 = 0.76$) but not with Caco-2 permeability ($r^2 = 0.29$). Correlations were also assessed between K_i/IC_{90} ratios and the following physico-chemical properties: log P ($r^2 = 0.41$), log D ($r^2 = 0.58$), c log P ($r^2 = 0.13$), and m log P ($r^2 = 0.30$). These results suggest that passive permeability may play a role in the uptake and cellular activity of these HCV protease inhibitors, and that PAMPA was more predictive of cellular activity than physico-chemical properties or Caco-2 permeability.

© 2007 Elsevier Inc. All rights reserved.

1. Introduction

Lead optimization of new chemical entities (NCEs) based on physico-chemical behavior plays a major role in modern drug discovery [1]. One of the primary goals during lead optimization is to identify compounds with reasonable membrane permeability. This property may ensure good oral absorption, acceptable CNS penetration, and sufficient target tissue uptake of the NCEs. Several cell-based and non-cell-based in vitro models have been established for membrane permeability screening [2]. Two of the most commonly used models are: the parallel artificial membrane permeability assay (PAMPA) system and the Caco-2 cell system [3,4]. PAMPA

was first demonstrated by Kansy et al. [5] as a high-throughput screening tool for predicting absorption. This model utilizes an artificial lipid membrane created by coating a hydrophobic filter with a mixture of lecithin/phospholipids dissolved in an inert organic solvent such as dodecane. Since then, several variants of PAMPA have been developed using different types of lipid barriers. PAMPA assesses passive diffusion of a molecule, the most common pathway for drug absorption and uptake by target tissues [6,7].

The Caco-2 cell system, usually performed in a Transwell device, measures permeability across the cells. For orally administered drugs, a sigmoidal relationship has been observed between percent of absorption and permeability

coefficients [8,9]. It is generally accepted that the permeability coefficient may also reflect the ability of a compound to passively permeate through the cell membrane. However, the Caco-2 cell has high level expression of P-glycoprotein and other active efflux transporters which would reduce the apical to basolateral permeability by pumping the substrates out of the cells. This type of efflux may under-estimate the potential of passive permeability of a compound.

The HCV RNA genome encodes a polyprotein of approximately 3000 amino acids, which is processed by host and viral proteases into structural and nonstructural (NS) polypeptides [10]. The NS3 protease is responsible for processing four cleavage sites of the nonstructural region. Non-natural synthetic polypeptides have been developed as potent competitive inhibitors for the HCV NS3 protease. A HCV protease inhibitor must first penetrate the liver cell membrane in order to reach its target, the HCV NS3 protease [11,12]. At Schering-Plough we use two different in vitro assays to evaluate the potency of potential HCV protease inhibitors. A cell-free system (continuous protease activity assay) monitors the inhibition of protease activity and generates intrinsic K_i values for NCEs, and a replicon assay using a Hu-7 cell line generates cell-based IC_{90} values [13]. Upon comparison, K_i and IC_{90} values for the same compound did not always correlate. One of the possible explanations for this lack of correlation is that different compounds may vary in cell membrane permeability. In this study we examined the cellular permeability of 34 novel HCV protease inhibitors using the Caco-2 and PAMPA systems and its relationship to the discordance between K_i and IC_{90} and to other physico-chemical properties.

2. Materials and methods

2.1. Reagents

Test compounds were synthesized within Schering-Plough Research Institute (Kenilworth, NJ). PAMPA lipid was obtained from pION Inc. (Woburn, MA; GIT-0 Lipid Solution) and was stored at −20 °C until use. A concentrated system solution and the acceptor sink buffer from pION Inc. were used as directed for dosing and receiving. A Multiscreen™ 96-well PVDF filter plate (pore size = 0.45 μm, surface area = 0.24 cm², porosity = 0.76 (units?)) and a transport receiver plate from Millipore Corporation (Billerica, MA) were used for PAMPA "sandwich" preparation. The Caco-2 cell line (passage 32–70) was obtained from the American Tissue Culture Collection (ATCC; Rockville, MD). Caco-2 permeability studies were performed using the HTS Multiwell™ insert system (Becton Dickinson Labware; Franklin Lakes, NJ) with PET membrane (24 wells, 1.0-μm pore size, 0.33-cm² surface area). All other chemicals were obtained from Sigma.

2.2. Methods

2.2.1. PAMPA permeability
Donor solution (10 μM) was prepared by diluting 1 mM DMSO compound stock solution using the diluted system buffer (pH adjusted to 7.4 with 1 M NaOH solution). Five microliters lipid solution was applied to each filter membrane. Donor solution

(200 μl) was added to each well of the filter plate. The filter plate was then put onto a receiver plate with 300 μl preloaded acceptor sink buffer. The sandwich was incubated at room temperature for 4 h. Samples were taken from both receiver and donor sides at the end of the incubation and analyzed using LC–MS/MS. Donor solutions were also analyzed for initial concentration.

2.2.2. Caco-2 cell culture and permeability
The cells were maintained in culture medium consisting of Dulbecco's Modified Eagle Medium (DMEM) supplemented with 10% fetal bovine serum (FBS), 1% non-essential amino acids, 2 mM L-glutamine, and 0.1% penicillin-streptomycin. Cells were maintained in an incubator at 37 °C with 5% CO_2 and 90% relative humidity. The cells were subcultured at 70–80% confluency by treatment with 0.25% trypsin containing EDTA.

For transport experiments, Caco-2 cells were seeded at a density of 60,000 cells/cm² onto a HTS Multiwell™ insert system with PET membranes. Plates were incubated at 37 °C with 5% CO_2 and 90% relative humidity. The medium was changed every 24 h using a Brandel cell culture automation system (Gaithersburg, MD). The cells were grown 21–25 days in the plate prior to the transport studies. The cell membrane integrity was measured by testing the ^{14}C-mannitol permeability for one plate from each batch using a Packard MultiProbe II system (Packard BioScience; Meriden, CT). The ^{14}C-mannitol permeability ranged from 5 to 8 nm/s. In addition, the cell membrane and monolayer integrity were verified by measuring the transepithelial electrical resistance (TEER) across each well both before and after transport experiments. TEER readings for each well ranged from 300 to 540 Ω cm².

Prior to the study, culture medium was removed from both the apical (AP) and basolateral (BL) wells, and then the wells were washed twice with warmed Hanks' Balanced Salt Solution (HBSS). The AP wells were replenished with 0.4 ml in HBSS buffer containing 10 mM MES and 10 mM D-glucose at pH 6.5 containing 10 μM of each compound. The BL wells were replenished with 1.0 ml HBSS buffer containing 10 mM HEPES, 10 mM D-glucose with 4% BSA (pH 7.4). Samples were taken after a 2-h incubation from both the donor and BL, receiver wells. The samples were analyzed using LC–MS/MS. Permeability for both PAMPA and Caco-2 was calculated by measuring the accumulated amount of a compound transported from donor side to receiver side as a function of time:

$$P_{app} = \frac{dM/dt}{C_0 S}$$

where C_0 was the initial compound concentration, S was the surface area of the membrane on the filter insert, M was the amount of compound transported to the receiver side at measuring time point (t). For PAMPA, filter area times porosity was used for S.

2.2.3. Protease activity assay
Recombinant proteases were tested using a chromogenic assay. The assays were performed at 30 °C in 96-well microtiter plates. One hundred microliters protease stock solution was added to 100 μl of assay buffer (25 mM MOPS, pH 6.5, 20% glycerol, 0.3 M

NaCl, 0.05% lauryl maltoside, 5 μM EDTA, 5 μM DTT) containing chromogenic substrate, Ac-DTEDVVP(Nva)-O-PAP, based on the NS5A carboxyl terminus coupled to p-nitrophenol. The reactions were monitored at an interval of 30 s for 1 h for change in absorbance at 370 nm using a Spectromax Plus microtiter plate reader (Molecular Devices). To determine enzyme concentration to be used in the assay, proteases were tested (1.6–100 nM) to achieve ∼12% substrate depletion over the course of the assay. To evaluate kinetic parameters of recombinant proteases, a range of substrate concentrations (0.293–150 μM) was used. Initial velocities were determined using linear regression, and kinetic constants were obtained by fitting the data to the Michaelis–Menton equation using MacCurveFit (Kevin Raner Software). Turnover rates were then calculated using the nominal enzyme concentration (2–9 nM). To assess the potency of protease inhibitors, the inhibition constants were determined at fixed concentrations of enzyme (2–9 nM) and substrate (40 μM). The data were fitted to the two-step slow-binding inhibition model: $P = v_s t + (v_0 - v_s)(1 - e^{-kt})/k$ using SAS (SAS Institute Inc.). The overall inhibition constant $K_i^* (v_s = V_{max}S/(K_m(1 + I/K_i^*)))$ was used to measure inhibitor potency.

2.2.4. Replicon concentration-response studies

To measure concentration-response, replicon cells were seeded at 4000 cell/well in 96-well collagen I-coated Biocoat plates (Becton Dickinson). Twenty-four hours post-seeding, protease inhibitors were added to replicon cells. The final concentration of DMSO was 0.5%, fetal bovine serum was 5%, and G418 was 500 μg/ml. Media and inhibitors were refreshed daily for 3 days, at which point the cells were washed with PBS and lysed in 1× cell lysis buffer (Ambion cat #8721). The replicon RNA level was measured using real time PCR (Taqman assay). The amplicon was located in NS5B. The PCR primers were: 5B.2F, ATGGACAGGCGCCCTGA; 5B.2R, TTGATGGG-CAGCTTGGTTTC. The probe sequence was FAM-labeled CACGCCATGCGCTGCGG. GAPDH RNA was used as endogenous control and was amplified in the same reaction as NS5B

(multiplex PCR) using primers and a VIC-labeled probe recommended by the manufacture (PE Applied Biosystem). The real-time RT-PCR reactions were run on an ABI PRISM 7900HT Sequence Detection System using the following program: 48 °C for 30 min, 95 °C for 10 min, and 40 cycles of 95 °C for 15 s, 60 °C for 1 min. The ΔCT values $(CT_{NS5B} - CT_{GAPDH})$ were plotted against drug concentration and fitted to the sigmoid dose response model using SAS (SAS Institute Inc.) or Graphpad PRISM software (Graphpad Software Inc.). IC$_{50}$ was the drug dose necessary to achieve ΔCT = 1 over the projected baseline. IC$_{90}$ was the drug dose necessary to achieve ΔCT = 3.2 over the baseline.

2.2.5. Physico-chemical parameters

The log D-pH 7.4 and log P-neutral form for the compounds were calculated using ACD/Labs version 7.06 (Toronto, Ontario) and the c log P and m log P were calculated by Sybyl 7.3 (Tripos Inc., St. Louis, MO) which uses version 4.3 c log P algorithm from Biobyte Corp (Claremont, CA).

3. Results

3.1. Structural classes of the HCV protease inhibitors

A total of 34 novel HCV protease inhibitors were randomly selected for this study. Chemical syntheses and characterization of other similar protease inhibitor compounds have been reported previously [14–16]. These 34 compounds are potent tetrapeptide/pentapeptide HCV NS3 protease inhibitors. They are divided into six structural classes of carbamates, esters, and acids (Table 1). They include three t-butyl-carbamates, three other carbamates, five $tert$-butyl esters, seven benzyl-esters, five alkyl- and cycloalkyl-esters, and eleven acids. A typical structure of the HCV protease inhibitor is shown in Table 1(a). In the P1 position, the most common moiety is n-valine with a cyclo-propyl side chain replacement. The

Table 1 – Structure of carbamates, esters, and acids			
Compound	P1	P1′	P4
(a) Structure of $tert$-butyl carbamate HCV inhibitors			
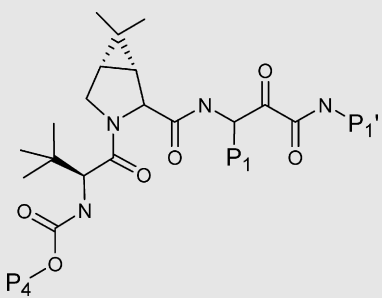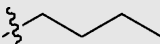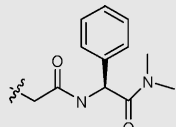
Table 1 (*Continued*)

Compound	P1	P1′	P4
2			
3		H	

Compound	P3	P1′	P2	P4

(b) Other carbamates

Compound		P1′		P3
4				
5				
6				

Compound	P1	P1′	P3

(c) *tert*-Butyl esters

Compound		P1′		P3
7		H		
8		H		

Table 1 (*Continued*)

Compound	P1	P1′	P3
9			
10			
11			

(d) Benzyl esters

Compound	P1	P1′	P4	R	R1
12		H		H	H
13				H	H
14				H	H
15		H		H	H
16		H		H	H
17		H		H	F
18				Me	H

Compound	P1	P1′	P4	R

Table 1 (*Continued*)

Compound	P1	P1′	P4	R

(e) Alkyl and cycloalkyl esters

Compound	P1	P1′	P4	R
19	(n-butyl)	allyl	(t-Bu)	(isopropyl)
20	(cyclopropylmethyl)	H	(t-Bu)	(indanyl)
21	(cyclopropylmethyl)	H	(t-Bu)	(cyclopentyl)
22	(cyclopropylmethyl)	H	(t-Bu)	(methylcyclopentyl)
23	(cyclopropylmethyl)	H	(t-Bu)	(cyclohexyl)

Compound	P1	P1′	P4	P3

(f) Acids

Compound	P1	P1′	P4	P3
24	(cyclopropylmethyl)	H	(isopropyl)	(t-Bu)
25	(cyclopropylmethyl)	(phenyl-N-methyl amide)	(sec-butyl)	(t-Bu)
26	(cyclopropylmethyl)	(phenyl-N-methyl amide)	(isobutyl)	(t-Bu)
27	(cyclopropylmethyl)	H	(isobutyl)	(t-Bu)
28	(cyclopropylmethyl)	H	(t-Bu)	(indanyl)

Table 1 (*Continued*)

Compound	P1	P1′	P4	P3
29		H		
30		H		
31				
32				
33				
34				

common P2 position contains a modified proline residue, and the P3 contains a *tert*-butyl or an indanylglycine group. Most of the structural variations located on the left side of the compounds are in the P4 and the capping groups (R and R1), while structural variations on the right side of the compounds are in the P1 and P1′ positions.

3.2. Determination of K_i

All of the above NS3 protease inhibitors were tested in a HCV protease continuous assay as described in Section 2.2 using the NS4A-tethered single-chain NS3 serine protease. The K_i values from the assay reflect the equilibrium constant determined by the reversible covalent bond formed between the ketone and serine as well as other interactions between the inhibitor and the protease. K_i values for these 34 compounds ranged from 0.003 to 0.3 μM-representing a two order of magnitude activity range. Larger inhibitors displayed greater intrinsic potency since they provide more structural interaction with the protease. Most of the acids were as potent as their ester counterparts, indicating the negative charge of the carboxylic moiety may not affect the affinity between the compound and the protease. This was further confirmed by X-ray crystallography and structure modeling, which showed that the acids display equal binding interaction in the active site of the NS3 protease (data not shown).

3.3. Determination of IC_{90}

The replicon cell-based assay is a functional assay for evaluating the potency of HCV protease inhibitors in inhibiting the subgenomic RNA replication. The IC_{90} of the compounds tested in this study ranged from 0.1 to 18 μM. In general, the acids were less active than their corresponding esters in the replicon cell-based assay. The esters appeared to be stable since no hydrolytic products were detected in the medium. In

addition, excessive amounts of the compounds were provided in the medium to ensure that protein binding will not affect the determination of IC_{90}.

3.4. K_i/IC_{90} ratio

As shown in Table 2, the K_i/IC_{90} ratio varied from compound to compound, indicating that intrinsic potency against the protease did not correlate well with their cell-based activities. This may be due to differences in intracellular compound concentrations. Attempts to quantify the intracellular compound concentrations in the replicon assay by LC/MS have failed, possibly due to insufficient intracellular levels.

3.5. Permeability in PAMPA and Caco-2 systems

The permeability coefficients of the 34 compounds used in this study ranged from 0.6 to 825 nm/s. The general trend was that polar compounds such as acids had lower permeability, whereas hydrophobic compounds, such as esters and carbamates, had higher permeability in the PAMPA system. The permeability coefficients in the Caco-2 system ranged from 1 to 101 nm/s. All six structural classes showed low-to-moderate permeability in the Caco-2 system. When the permeability in PAMPA was compared with that of Caco-2, no obvious correlation was observed ($r^2 = 0.10$).

3.6. Determination of log P, log D, c log P, and m log P

Table 2 shows the physico-chemical properties of these 34 compounds. Values for log P range from 0.26 to 5.69, c log P range from 3.26 to 7.69, and m log P range from 0.69 to 2.83. No apparent difference was noted between the acids and the neutral compounds, such as esters and carbamates, for these properties. Values for log D, however, clearly separate the acids from other neutral compounds. Values for log D range

from −1.99 to 5.69. All acids have negative $\log D$ values, whereas esters and carbamates have positive $\log D$ values (Table 1).

3.7.   Linear regression analysis of correlation

Linear regression analysis was performed to evaluate the relationship between K_i/IC_{90} and PAMPA permeability. A high r^2 value (0.76, $p < 0.05$) was observed between these two parameters, suggesting a statistically reasonable correlation exists (Fig. 1a). A fairly low r^2 value (0.29) was found between K_i/IC_{90} and Caco-2 permeability, indicating a lack of correlation between these two parameters. Low to moderate r^2 values were observed between K_i/IC_{90} and other physico-chemical parameters: $\log P$ ($r^2 = 0.41$), $\log D$ ($r^2 = 0.58$), $c \log P$ ($r^2 = 0.13$), and $m \log P$ ($r^2 = 0.30$) (Fig. 1). Overall, the correlation between K_i/IC_{90} and PAMPA permeability seems to be the highest. A separate linear regression analysis plotting IC_{90} against PAMPA permeability/K_i ratio also showed very good correlation with $r^2 = 0.67$ (Fig. 2), indicating that IC_{90} could be predicted by the PAMPA permeability after normalized by the K_i value.

Since both PAMPA and $\log D$ show reasonable correlation scores, a new linear regression analysis was performed by excluding the acid compounds (Fig. 3(a) and (b)). Despite the much narrow dynamic range of the K_i/IC_{90} ratio, the correlation between the PAMPA and the K_i/IC_{90} ratios of the remaining 23 non-acid compounds appears to be moderate with $r^2 = 0.39$. There appears to be no correlation between $\log D$ and K_i/IC_{90} ration since the $r^2 = 0.001$.

4.   Discussion

Cell uptake represents an essential process for a drug to enter the target tissue. The drug needs to posses some degree of membrane permeability in order to be orally absorbed and to penetrate the cell membrane. Membrane permeability is a complex phenomenon which may involve passive diffusion, active transport via drug transporters and endocytosis. For many peptides and peptidomimetics drug candidates, such as the HCV protease inhibitors, the membrane permeability may present a major obstacle for achieving oral absorption and potency in target tissues. Strategies designed to improve the

Table 2 – K_i^*, IC_{90}, K_i^*/IC_{90} ratio, PAMPA permeability, Caco-2 permeability, $\log P$-neutral form, $\log D$-pH 7.4, $c \log P$ and $m \log P$ of 34 novel HCV protease inhibitors

| Compound	Molecular weight	HCV K_i^* (nM)	Replicon IC_{90} (µM)	K_i/IC_{90} ratio	PAMPA perm (nm/s)	Caco-2 perm (nm/s)	log P-neutral form	log D-pH 7.4	c log P	m log P
1	727	10	0.4	0.025	66 ± 4	54 ± 7	4.19	4.19	5.78	1.40
2	713	14	0.25	0.056	61 ± 9	41 ± 10	3.66	3.65	5.25	1.23
3	620	30	0.4	0.075	300 ± 95	47 ± 3	3.34	3.34	4.67	1.64
4	745	19	2.0	0.009	152 ± 43	20 ± 3	3.54	3.54	5.39	0.70
5	743	10	1.8	0.005	125 ± 31	11 ± 0.2	3.83	3.83	4.86	0.70
6	739	10	0.2	0.050	86 ± 19	27 ± 0.2	4.67	4.67	6.27	1.58
7	680	18	0.4	0.045	158 ± 15	42 ± 9	4.33	4.33	5.14	2.31
8	694	20	10.0	0.002	26 ± 15	35 ± 5	4.89	4.89	5.7	2.49
9	724	110	0.3	0.366	289 ± 68	93 ± 5	5.62	5.62	7.9	2.83
10	724	300	14	0.021	129 ± 94	101 ± 6	5.69	5.69	7.98	2.83
11	662	50	0.1	0.500	595 ± 126	170 ± 4	5.02	5.02	7.28	2.11
12	654	290	3.4	0.085	535 ± 60	37 ± 2	3.78	3.78	4.93	1.96
13	872	300	3.1	0.096	824 ± 56	3 ± 0.7	3.96	3.96	5.15	1.96
14	872	12	0.4	0.030	777 ± 63	1.5 ± 0.3	5.07	5.06	7.26	1.63
15	654	6	0.5	0.012	31 ± 11	5.2 ± 4	5.07	5.06	7.26	1.63
16	654	68	0.4	0.170	295 ± 29	31 ± 1.8	3.96	3.96	5.15	1.96
17	672	15	0.1	0.150	443 ± 14	36 ± 8	3.83	3.83	5.16	2.32
18	710	110	4.7	0.023	323 ± 96	117 ± 3	5.99	5.99	8.06	2.59
29	648	38	0.8	0.047	649 ± 17	117 ± 4	4.67	4.67	6.88	1.93
20	680	30	0.5	0.060	321 ± 18	48 ± 9	4.25	4.25	5.29	2.31
21	632	41	0.8	0.051	451 ± 16	45 ± 15	3.43	3.43	4.78	1.83
22	646	70	1.3	0.053	97 ± 16	70 ± 6	3.92	3.92	5.3	2.01
23	646	80	2.7	0.029	151 ± 21	41 ± 0.5	3.99	3.99	5.34	2.01
24	564	24	18.0	0.001	1 ± 0.1	3 ± 1	1.47	−1.69	3.04	0.87
25	782	3	10.0	0.0003	0.7 ± 0.1	1.2 ± 0.1	0.26	−1.99	5.38	0.69
26	782	5	5.0	0.0010	0.6 ± 0.1	42 ± 8	0.26	−1.99	5.38	0.69
27	624	100	20.0	0.0050	12 ± 8	13 ± 6	1.65	−1.55	3.26	0.87
28	638	7	4.1	0.0017	0.7 ± 0.1	1 ± 0.1	2.64	−0.58	3.73	1.59
29	638	8	5.0	0.0016	1.0 ± 0.2	2 ± 1	3.2	−0.015	4.29	1.78
30	564	12	3.2	0.0037	0.9 ± 0.1	20 ± 7	1.65	−1.55	3.26	0.87
31	654	57	20.0	0.0028	1.4 ± 0.1	50 ± 8	3.58	0.38	6.18	1.96
32	668	35	3.5	0.0100	4.2 ± 2	53 ± 3	3.93	0.73	6.49	2.14
33	668	74	20.0	0.0037	7.8 ± 2	5 ± 0.9	4.00	0.8	6.57	2.14
34	606	20	10.0	0.0020	0.7 ± 0.1	38 ± 7	3.33	0.13	5.87	1.37
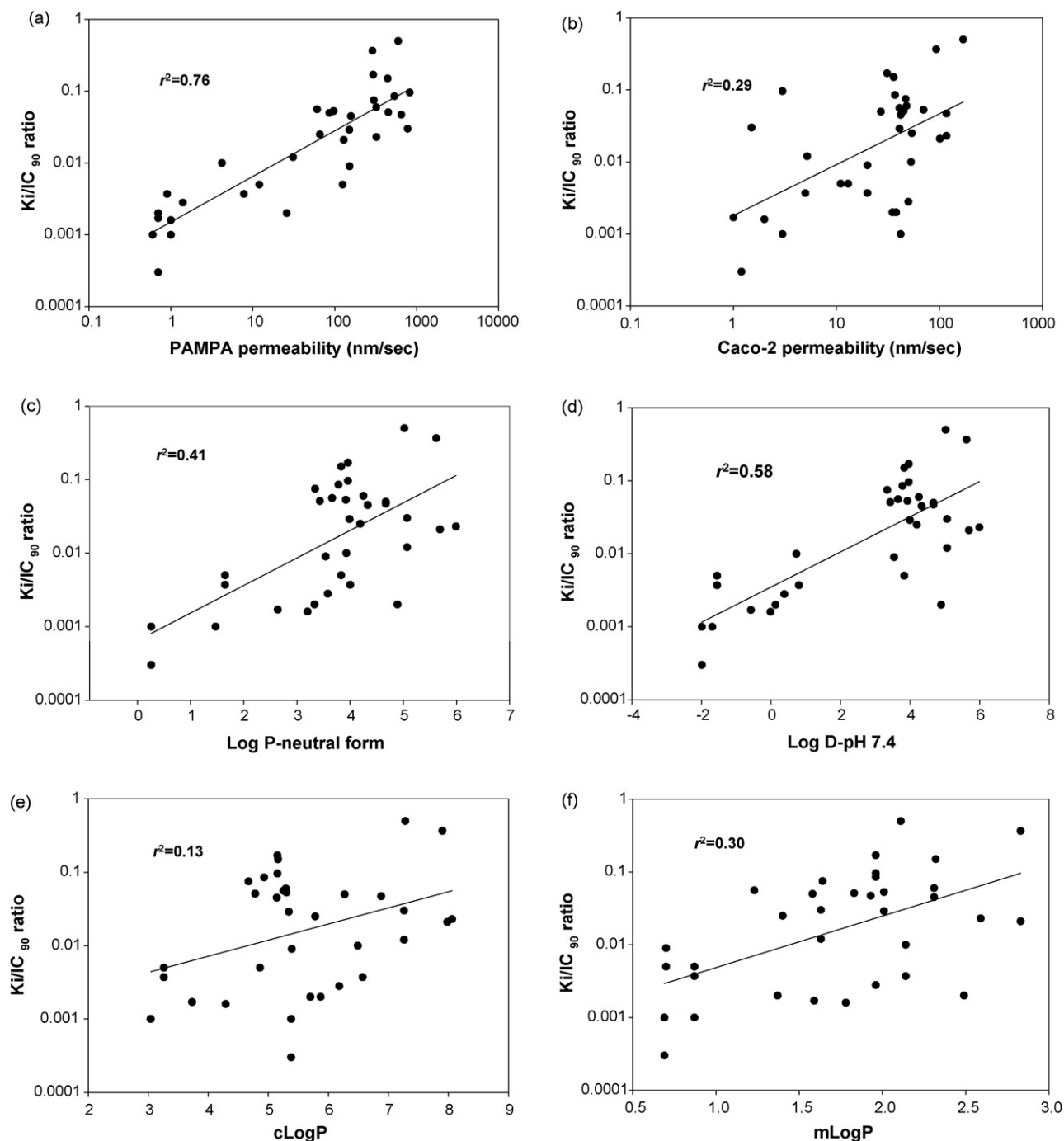
Fig. 1 – (a) Linear regression analysis of correlation between K_i/IC_{90} ratio and PAMPA permeability. (b) Linear regression analysis of correlation between K_i/IC_{90} ratio and Caco-2 permeability. (c) Linear regression analysis of correlation between K_i/IC_{90} ratio and log P-neutral form. (d) Linear regression analysis of correlation between K_i/IC_{90} ratio and log D-pH 7.4. (e) Linear regression analysis of correlation between K_i/IC_{90} ratio and c log P. (f) Linear regression analysis of correlation between K_i/IC_{90} ratio and m log P.

membrane permeability of these types of compounds have emphasized on optimizing specific physico-chemical properties to facilitate permeability; these approaches includes improving lipophilicity, reducing molecular size, reducing charge state, and increasing solubility [17,18]. Since permeability in the gastrointestinal tract may be mediated through paracellular (via tight-junction) or transporter(s), there may be compounds with reasonable intestinal permeability, yet lacking the passive permeability which is required for uptake by the target tissue/cells.

Many in vitro systems have been employed for the understanding of the underlying mechanism(s) of membrane
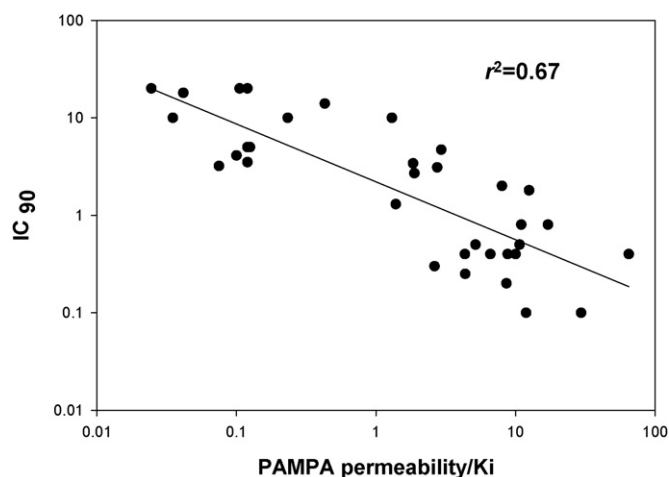
Fig. 2 – Linear regression analysis of correlation between IC_{90} and PAMPA permeability/K_i of HCV protease inhibitors.

permeability. For example, the Caco-2 cell system is a very common tool for evaluation of cellular permeability. During the differentiation process in Caco-2 cell culture which leads to formation of tight junctions and development of cell polarity, various drug transporters are also expressed in a polarized manner. It is well documented that the major efflux pumps, such as P-glycoprotein (P-gp) and breast cancer resistant protein (BCRP), are highly expressed in Caco-2 cells [19,20]. The presence of these transporters may be valuable when the in vitro data are used to correlate with the in vivo uptake by tissues, such as the brain, since the blood–brain barrier also shows high expression of P-gp and other efflux transporters. On the other hand, if the target tissue lacks the expression of the transporters, the cell permeability observed in the Caco-2 cell may not accurately translate into cell permeability/uptake.

In contrast to the Caco-2 system, the PAMPA system represents a more simple passive permeability model. Its utility has been suggested in predicting human absorption, as a screening model for blood–brain barrier permeability and as a model for evaluating the skin permeability [21–23]. In a recent commentary, it indicated that PAMPA is suitable for categorizing compounds into high versus low permeability bins, but the same outcome could be achieved by using calculated log D-pH 7.4 [24]. In a rebuttal commentary it indicated that PAMPA is a relative new tool in drug discovery and the complexity of the passive membrane permeability could be easily underestimated [25]. It is recognized that both PAMPA and Caco-2 system may be potentially useful tools in evaluating the membrane permeability of a compound, yet the Caco-2 system represents a more complex system due to the presence of efflux and uptake transporters expressed in the cell in a polarized manner. For example, a P-glycoprotein substrate may display high permeability in the PAMPA and low in the Caco-2 system due to the efflux. Hence, the different in the permeability in PAMPA and the Caco-2 system for the 34 HCV protease inhibitors may also reflect the fact that these HCV protease inhibitors may be P-glycoprotein substrates (data not shown). In our laboratory, both PAMPA and the Caco-
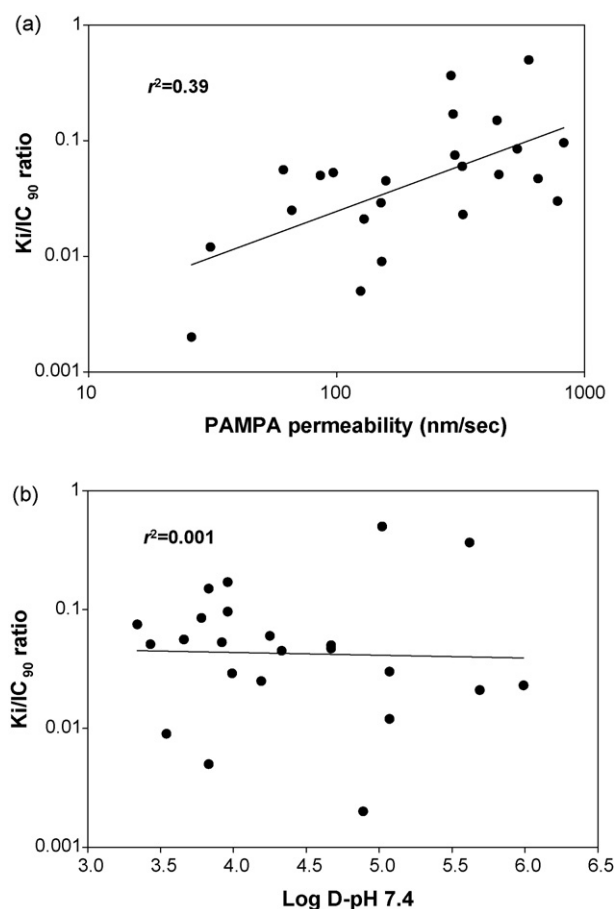

Fig. 3 – (a) Linear regression analysis of correlation between K_i/IC_{90} and PAMPA permeability of HCV protease inhibitors excluding acids. (b) Linear regression analysis of correlation between K_i/IC_{90} and log D-pH 7.4 of HCV protease inhibitors excluding acids.

2 system are validated [1]. The difference observed in this study between these two systems is not due to experimental error.

In the liver, the cellular uptake could be mediated by passive diffusion and/or active transport via the uptake transporters, such as OATPs [26]. Chemically blocking of OATPs activity using inhibitors, such as rifampicin, may reduce the uptake as evidenced by the decrease of liver levels of the OATP substrate in rats [27]. Although the uptake/penetration of the liver is generally considered less restricted than other tissues, such as the brain, it has not been well-examined in terms of the permeability of peptide compounds. A recent study has demonstrated that uptake could be a rate-limiting step for drug metabolism in the liver [28]. Hence, the uptake could also become a rate-limiting step for a drug candidate to reach the intracellular target and for the cellular activity.

In this study we also intended to understand the relationship between cellular activity and the physico-chemical properties using a set of HCV protease inhibitors. As shown in the results, there is only moderate correlation between the cellular activity and log D, indicating that the negative charge

may have some effect of the membrane permeability. Likewise, a moderate correlation between the cellular activity and log P suggests that hydrophobicity of the compound may only partially predict the membrane permeability. It is possible that one needs to combine multiple physico-chemical properties into a single parameter for better prediction of membrane permeability of a given compound. One of the potential interesting aspects of these types of compounds is relevant of solute–solvent hydrogen-bonds. The free energy required to desolvate a peptide inversely correlates with the permeability of the peptide [29]. For example, peptides with a well-defined secondary structure, such as β-turn, may exhibit intramolecular hydrogen-bond, which reduces the hydrogen-bonding potential with the solvent. Understanding of this type of intramolecular inter-action would aid future design of molecules with improved membrane permeability.

Nevertheless, we have shown a reasonable correlation between the PAMPA permeability and the cell-based activity of 34 HCV protease inhibitors. Low-to-moderate correlation was found between the cell-based activity and 1. Caco-2 permeability and 2. physico-chemical properties such as log P, c log P, log D, and m log P. These results suggest that HCV protease inhibitors are taken up by the cell through passive diffusion and that PAMPA represents a good in vitro model for evaluation of their permeability.

REFERENCES

[1] Li C, Wainhaus S, Uss AS, Cheng K-C. High-throughput screening using Caco-2 and PAMPA systems. In: Kim K-J, Ehrhardt C, editors. Preclinical biopharmaceutics—in situ, in vitro, and in silico tools for drug absorption studies. Springer; 2007. p. 418–29.

[2] Balimane PV, Chong S, Morrison RA. Current methodologies used for evaluation of intestinal permeability and absorption. J Phamacol Toxicol Methods 2000;44:301–12.

[3] Artursson P. Cell cultures as models for drug absorption across the intestinal mucosa. Crit Rev Ther Drug Carrier Syst 1991;8:305–30.

[4] Chong S, Dando S, Soucek K, Morrison RA. In vitro permeability through caco-2 cells is not quantitatively predictive of in vivo absorption for peptide-like drugs absorbed via the dipeptide transporter system. Pharm Res 1996;13:120–3.

[5] Kansy M, Senner F, Gubermator K. Physicochemical high throughput screening: parallel artificial membrane permeation assay in the description of passive absorption processes. J Med Chem 1998;41:1007–10.

[6] Avdeef A, Strafford M, Block E, Balogh MP, Chabliss W, Khan I. Drug absorption in vitro model: filter-immobilized artificial membranes. 2. Studies of the permeability properties of lactones in Piper methysticum Forst. Eur J Pharm Sci 2001;14:271–80.

[7] Avdeef A. Absorption and drug development. New York, NY: Wiley-Interscience; 2003. p. 116–246.

[8] Chong S, Dando S, Morrison RA. Evaluation of Biocoat intestinal epithelium differentiation environment (3-day cultured Caco-2 cells) as an absorption screening model with improved productivity. Pharm Res 1997;14:1835–7.

[9] Rubas W, Jezyk N, Grass GM. Comparison of the permeability characteristics of a human colonic epithelial (Caco-2) cell line to colon of rabbit, monkey, and dog

intestine and human drug absorption. Pharm Res 1993;10:113–8.

[10] Reed KE, Rice CM. Overview of hepatitis C virus genome structure, polyprotein processing, and protein properties. Curr Top Microbiol Immunol 2000;242:55–84.

[11] Lamarre D, Anderson PC, Bailey M, Beaulieu P, Bolger G, Bonneau P, et al. An NS3 protease inhibitor with antiviral effects in humans infected with hepatitis C virus. Nature 2003;426:186–9.

[12] Cheng K-C, Korfmacher WA, White RE, Njoroge FG. Lead optimization in discovery drug metabolism and pharmacokinetics: case study—the hepatitis C virus protease inhibitor SCH 503034. Perspect Med Chem 2007;1:1–9.

[13] Liu R, Abid K, Pichardo J, Pazienza V, Ingravallo P, Kong R, et al. In vitro antiviral activity of SCH446211 (SCH6), a novel inhibitor of the hepatitis C virus NS3 serine protease. J Antimicrob Chemother 2006;10:1093–8.

[14] Chen KX, Njoroge FG, Arasappan A, Venkatraman S, Vibulbhan B, Yang W, et al. Novel potent hepatitis C virus NS3 serine protease inhibitors derived from proline-based macrocycles. J Med Chem 2006;49:995–1005.

[15] Bogen SL, Arasappan A, Bennett F, Chen K, Jao E, Liu Y-T, et al. Discovery of SCH6: a new ketoamide inhibitor of the HCV NS3 serine protease and HCV subgenomic RNA replication. J Med Chem 2006;49:2750–7.

[16] Venkatraman S, Bogen SL, Arasappan A, Bennet F, Chen K, Jao E, et al. Discovery of SCH 503034, a selective potent, orally bioavailable HCV NS3 protease inhibitor: a potential therapeutic agent for the treatment of hepatitis C infection. J Med Chem 2006;49:6074–86.

[17] Burton PS, Conradi RA, Ho NFH, Hilgers AR, Borchardt RT. How structural features influence the biomembrane permeability of peptides. J Pharm Sci 1996;85:1336–40.

[18] Knipp GT, Vander Velde DG, Siahaan TJ, Borchardt RT. The effect of β-turn structure on the passive diffusion of peptides across Caco-2 cell monolayers. Pharm Res 1997;14:1332–40.

[19] Adachi Y, Suzuki H, Sugiyama Y. Comparative studies on in vitro methods for evaluating in vivo function of MDR1 P-glycoprotein. Pharm Res 2001;18:1660–8.

[20] Breedveld P, Beijnen JH, Schellens JH. Use of P-glycoprotein and BCRP inhibitors to improve oral bioavailability and CNS penetration of anticancer drugs. Trends Pharmacol Sci 2006;27:17–24.

[21] Ottaviani G, Martel S, Carrupt P-A. Parallel artificial membrane permeability assay: a new membrane for the fast prediction of passive human skin permeability. J Med Chem 2006;49:3948–54.

[22] Loftsson T, Konradsdottir F, Masson M. Development and evaluation of an artificial membrane for determination of drug availability. Int J Pharm 2006;326:60–8.

[23] Fischer H, Kansy M, Avdeef A, Senner F. Permeability of permanently positive charged molecules through artificial membranes-influence of physico-chemical properties. Eur J Pharm Sci 2007;31:32–42.

[24] Galinis-Luciani D, Nguyen L, Yazdanian M. Is PAMPA a useful tool for discovery. J Pharm Sci 2007;96:2886–92.

[25] Avdeef A, Bendels S, Di L, Faller B, Kansy M, Sugano K, et al. PAMPA-critical factors for better prediction of absorption. J Pharm Sci 2007;96:2893–909.

[26] Rassetto LA, Poon S, Tsourounis C, Valera C, Benet LZ. Effects of uptake and efflux transporter inhibition on erythromycin breath test results. Clin Pharmacol Ther 2007;81:828–32.

[27] Lau YY, Huang Y, Frassetto L, Benet LZ. effect of OATP1B transporter inhibition on the pharmacokinetics of atorvastatin in healthy volunteers. Clin Pharmacol Ther 2007;81:194–204.

[28] Lu C, Li P, Gallegos R, Uttamsingh V, Xia CQ, Miwa GT, et al. Comparison of intrinsic clearance in liver microsomes and hepatocytes from rats and humans: evaluation of free fraction and uptake in hepatocytes. Drug Metab Dispos 2006;34:1600–5.

[29] Gangmar S, Jois SDS, Siahaan TJ, Vander Velde DG, Stella VJ, Borchardt RT. The effect of conformation on membrane permeability of an acyloxlalkoxy-linked cyclic prodrug of a model hexapeptide. Pharm Res 1996;13: 1657–62.